Ion Conduction and Selectivity in K+ Channels

Benoît Roux

Department of Physiology and Biophysics, Weill Medical College of Cornell University, New York, NY 10021; email: benoit.roux@med.cornell.edu

Key Words   molecular dynamic simulations, KcsA, free energy, potential of mean force, crystallographic B-factors, gating

■ **Abstract**   Potassium (K^+) channels are tetrameric membrane-spanning proteins that provide a selective pore for the conductance of K^+ across the cell membranes. These channels are most remarkable in their ability to discriminate K^+ from Na^+ by more than a thousandfold and conduct at a throughput rate near diffusion limit. The recent progress in the structural characterization of K^+ channel provides us with a unique opportunity to understand their function at the atomic level. With their ability to go beyond static structures, molecular dynamics simulations based on atomic models can play an important role in shaping our view of how ion channels carry out their function. The purpose of this review is to summarize the most important findings from experiments and computations and to highlight a number of fundamental mechanistic questions about ion conduction and selectivity that require further work.

## CONTENTS

PERSPECTIVE AND OVERVIEW

The determination of the structure of the bacterial KcsA channel from *Streptomyces lividans* in 1998 by MacKinnon and coworkers offered the first view of the general architecture of these proteins (39) (Figure 1, see color insert). Because KcsA is structurally similar to eukaryotic K^+ channels, investigations of KcsA are expected to help researchers understand a large class of biologically important channels. The X-ray structure of KcsA triggered a large number of computational studies based on molecular dynamics (MD) (4, 6, 7, 16, 17, 21, 25, 26, 29, 31, 36, 38, 54, 55, 82, 83, 84, 103, 118, 119), Poisson-Boltzmann (PB) dynamics (108, 113, 114), and Brownian dynamics (BD) (5, 22, 23, 91). Because of the moderate resolution of the X-ray data (3.2 Å), the computational studies initiated from the original 1998 KcsA structure proceeded with a limited amount of information. In particular, the exact number and configurations of the ions and water molecules in the selectivity filter were not known, and whether the channel was in an open or closed state in the crystal structure was unclear. The picture was rapidly refined during the following few years as additional structural and functional information became available. X-ray structures of the KcsA channel were obtained at higher resolution (up to 2.0 Å) (95, 132, 135), followed by structures for other K^+ channels: MthK (3.4 Å), a calcium-activated channel crystallized in an open state (68); KvAP (3.2 Å), a voltage-gated channel (70); and KirBAC (3.6 Å), an inward rectifier (77). Further information about the molecular movements of the transmembrane helices of KcsA and their role in channel gating was obtained by electron spin resonance (ESR) (30, 32, 51, 52, 80) and mass spectroscopy (75). At the same time, the results of electrophysiological experiments on KcsA became available (59, 78, 79, 102). In retrospect, it is encouraging that many results from the computational studies have been consistent with the rapidly emerging data, sometimes even in advance of the fact (93). A number of factors have contributed to the recent success of the computational studies on biological membrane channels: clearly posed conceptual challenges, suitability of simulation timescales, availability of high-resolution structures, and opportunities for experimental verification (115).

Several excellent reviews covering computational studies of ion channels have been published in the past few years. A number of them have provided timely and critical summaries of the most important results from simulation studies (37, 94, 111, 115, 116), structural modeling (49, 116), and bioinformatics sequence analysis approaches (24, 117). A few have focused specifically on the general methodologies used in computational studies of ion channels (28, 112, 123) (for more about simulation methodologies, see References 2 and 13). The purpose of this review is to summarize important findings and to highlight a number of

fundamental mechanistic questions about ion conduction and selectivity that will require further work.

KEY MECHANISTIC QUESTIONS

One key mechanistic question about K^+ channels is how are they able to achieve a fast throughput rate and yet remain highly selective for K^+ over Na^+. More than 50 years ago, Hodgkin & Keynes (66) used radioactive flux marker experiments to show that the K^+ channel was a narrow pore containing two to three K^+ and that permeation involved single-file ion movements across the membrane. According to the "knock-on" mechanism that they proposed, the approach of one ion from one side of the pore is coupled to the simultaneous exit of an other ion on the opposite side of the pore,

$$K^+ \quad \underline{\quad K^+ \quad K^+ \quad} \quad \rightleftharpoons \quad \underline{\quad K^+ \quad K^+ \quad} \quad K^+$$
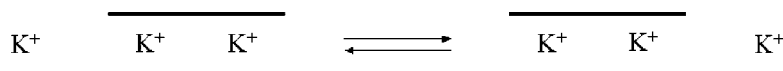
thereby enabling fast conduction. Over the following years, the notion of selective ion channels as narrow molecular "proteinaceous" pores and the steric constraints they put on permeation was refined, particularly through the work of Mullins (97, 98). But steric constraint did not explain how a pore could discriminate K^+ from Na^+, i.e., allow the passage of the larger cation and block the smaller one. A thermodynamic perspective on ion selectivity based on free energy differences, elaborated by Eisenman (40), clarified these matters considerably. Fundamentally, ion selectivity is controlled by the relative free energy of K^+ and Na^+ in the pore and in the bulk solution. In the early 1970s, Bezanilla & Armstrong (19) expanded on this idea of a narrow molecular pore and proposed the "snug-fit" hypothesis to explain the selectivity of K^+ channels: Na^+ ions do not enter the narrowest part of the pore because they are too small to fit well in the coordination cage provided by the channel as replacement for the water molecules surrounding the ion in solution. A different point of view was proposed by Eisenman and coworkers (120), who argued that the selectivity was more similar to the transfer process from water to an organic solvent. Detailed ion-flux experiments highlighted the high selectivity of K^+ channels (63) but could be consistent with both explanations.

The X-ray structure of KcsA determined in 1998 (39) is strikingly consistent with the classical views of a very selective, fast-conducting, multi-ion pore (Figure 1). The pore comprises a wide, nonpolar aqueous cavity on the intracellular side, leading up, on the extracellular side, to a narrow pore that is 12 Å long and lined exclusively by main chain carbonyl oxygens. Formed by the residues corresponding to the signature sequence TTVGYG, common to all K^+ channels (58), this region of the pore acts as a selectivity filter by allowing only the passage of nearly dehydrated K^+ ions across the cell membrane. The rate-limiting step in the conduction mechanism is expected to be the translocation of nearly dehydrated

K$^+$ ions in single file through the narrowest region of the pore. The latter appears to be well adapted to compensate for the dehydration of K$^+$ but not Na$^+$ ions. A single isolated K$^+$ ion would interact strongly with the carbonyl oxygens and remain tightly boundto the selectivity filter. But the presence of multiple K$^+$ results in mutual electrostatic repulsion directed alongthe axis of the narrow pore, which contributes to yield a high-throughput rate via a knock-on mechanism.

However, how selective conduction of K$^+$ ions takes place efficiently at the atomic level is complex. The knock-on mechanism assumes that ion-channel attraction and ion-ion repulsion play compensating effects, as several ions move simultaneously in single file through the narrow pore: The approach of one ion from one side of the (doubly occupied) selectivity filter is coupled to the simultaneous exit of an other ion on the opposite side. Although plausible, this mechanism relies on a strikingly delicate energy balance. To allow rapid ion conduction, the strong attraction between the ions and the channel must be exquisitely counterbalanced by the electrostatic repulsive forces between the ions. A simple calculation shows that the direct ion-ion coulombic repulsion could vary by several tens of kcal per moleculeduring the conduction process. Somehow, the K$^+$ channel exploits such large energies in a productive manner to yield a flux of approximately 10^8 ions per second. Fast conduction implies that there is no significant activation free energy barrier opposing the concerted ion translocation. How can this be possible?

How the channel achieves a high selectivity for K$^+$ over Na$^+$ is also a fascinating question. On the basis of the X-ray structure, it has been suggested that the filter is constrained in an optimal geometry by a network of aromatic residues surrounding the selectivity filterso that a dehydrated K$^+$ ion fits snugly with proper coordination by the backbone carbonyl oxygens, but that it cannot distort sufficiently to coordinate a smaller cation such as Na$^+$ (39, 135). It is almost taken for granted that the X-ray structure of KcsA confirmed the elegant mechanism of selectivity proposed by Bezanilla & Armstrong (19) (11, 12, 15, 22, 48, 65, 130, 135). However, this question is more complex than it appears to be. The atomic radius of K$^+$ and Na$^+$ differs only by 0.38 Å (106), implying that the snug-fit mechanism (19) relies on the ability of the selectivity filter to rigidly retain a remarkably precise (subangstrom) geometry to discriminate between these two cations. Proteins, like most biological macromolecular assemblies, are soft materials that display significant structural flexibility at room temperature (73). Despite some uncertainties, the B-factors of the KcsA channel indicate that the RMS fluctuations of the atoms lining the selectivity filter are on the order of 0.75 to 1.0 Å (Figure 2, see color insert), in general agreement with MD simulations of KcsA (4, 6, 7, 16, 17, 21, 29, 38, 54, 55, 82, 83, 103, 118, 119). The magnitude of atomic thermal fluctuations is fundamentally related to the intrinsic flexibility of a protein, i.e., how it responds structurally to external perturbations (3). These considerations suggest that, at room temperature, the channel should distort easily to cradle Na$^+$ with little energetic cost; this is seen in simulations with Na$^+$ in KcsA (21, 38, 54). The flexibility of the pore is further highlighted by the experimental observation that

K^+ is needed for the overall stability of the channel structure (76, 81, 92, 133, 135). Therefore, although the snug-fit hypothesis is consistent with a static view of the crystallographic structure, it does not jibe with the current knowledge of proteins. But then, what is the microscopic mechanism of selectivity?

ION CONDUCTION

The most fundamental mechanistic insight from MD simulations about the ion conduction through the KcsA channel is the concept of a single file of K^+ separated by water molecules dynamically moving through the narrowest region of the pore in a highly correlated fashion (4, 6, 7, 16, 17, 29, 38, 54, 55, 118, 119). One water molecule per K^+ is transported through the narrow pore (7, 16, 17), which is observed experimentally (1) and consistent with diffraction data (131). The selectivity filter is also where the driving force arising from the transmembrane electrostatic potential is predominant (18, 69, 113). The maximum electric conductance of K^+ through the selectivity filter of KcsA was calculated to be on the order of 300 to 500 pS (18), in agreement with experimental measurements (79).

Transport Cycle

The elementary events underlying the ion conduction process are best visualized with a transport cycle between multi-ion states. The transport cycle based on the computational studies is shown in Figure 3 (see color insert) (17, 18). The cycle bears many similarities to the classical knock-on mechanism of Hodgkin & Keynes (66) shown in Scheme 1. The conduction process, with alternatively two and three K^+ in the narrowest part of the pore, is similar to the knock-on mechanism (66) and is consistent with ion occupancy determined by X-ray diffraction at high resolution (131, 134, 135). At physiological concentrations the selectivity filter is predominantly occupied by two K^+ ions, in the configurations $[S_1, S_3]$ or $[S_2, S_4]$ (7, 39, 134, 135). At some point (e.g., during an outward conduction event), a third ion hops from the intracellular vestibular cavity into site S_4, while two ions in the selectivity filter are located in sites S_1 and S_3. The incoming ion induces a concerted transition to a state in which the three ions occupy sites S_4, S_2, and S_0, which is then followed by the rapid dissociation and departure of the outermost ions in S_0 on the extracellular side, yielding the conduction of one K^+.

A transport cycle was also elaborated by Morais-Cabral et al. (95) to describe the ion conduction mechanism. Like the ion conduction mechanism determined from the computation studies (Figure 3), this process is similar tothe classical knock-on mechanism of Hodgkin & Keynes (66) shown in Scheme 1; it pictures ion conduction as a collision between an incoming K^+ and the two ions located in the selectivity filter, resulting in the ejection of the ion at the opposite end of the pore. But a number of differences are also worth noting. Morais-Cabral et al. (95) stressed the importance of the energy balance between the configurations with two K^+, $[S_3,$

S_1] and [S_4, S_2]. The rate-limiting step is represented as an unfavorable activated complex with three equidistant K^+ located between the four cation binding sites of the selectivity filter, S_1, S_2, and S_4, and the transport cycle does not specifically involve other binding sites, such as the vestibular cavity or S_0. Such a high-energy activated complex with three K^+ is not observed in the computational studies (17). Instead, the key microscopic event underlying ion conduction is the concerted transition between the two stable low-energy configurations with three K^+, [cavity, S_3, S_1] and [S_4, S_2, S_0] (17). The two-ion configurations [S_1, S_3] and [S_2, S_4] have indeed roughly the same free energy (7), and the exchange rate between them is extremely rapid (4, 6, 7, 16, 17, 29, 38, 54, 55, 118, 119). But the back-and-forth shuttling of two K^+ in the selectivity filter, in the absence of a third K^+, does not control the throughput rate. The critical step leading to productive conduction involves configurations with three K^+ located within the vicinity of the pore, that is, the five main cation binding sites, S_0, S_1, S_2, S_3, and S_4, and the vestibular cavity. According to the computations, efficient knock-on is apparently made possible because the approach of an incoming ion on the intracellular side is not energetically prohibitive, whereas the dissociation of the outermost ion in S_0 is accelerated by ion-ion repulsion (17, 18). Although the computational results are consistent with available data, they have yet to be verified directly by experiments.

ION SELECTIVITY

The key question about selectivity is straightforward: What is the microscopic basis for the unfavorable free energy: $\Delta\Delta G(\text{Na}^+ \rightarrow \text{K}^+) = \left[G_{\text{pore}}(\text{Na}^+) - G_{\text{pore}}(\text{K}^+)\right] - \left[G_{\text{bulk}}(\text{Na}^+) - G_{\text{bulk}}(\text{K}^+)\right]$? By going beyond considerations based on static structures, researchers can use alchemical free energy perturbation (FEP) computations based on atomic models (2, 13) to help clarify the (often hidded) microscopic factors that govern thermodynamics. The results of FEP computations show that, indeed, occupancy by Na^+ in the selectivity filter is thermodynamically unfavorable (4, 7, 17, 83, 103), which is in good agreement with ion-flux measurements (101, 102). But these results present a clear paradox: The calculated free energies are consistent with a selective channel, but the thermal fluctuations of the backbone atoms lining the pore are obviously too large to be consistent with the snug-fit mechanism (19, 39). An alternative explanation might be that selectivity arises locally, from the intrinsic properties of the microscopic interactions taking place in the pore (40, 41, 120, 128).

Importance of Carbonyl-Carbonyl Repulsion

The most important interactions taking place in the first coordination shell around an ion in the pore are the very strong electrostatic attraction and core repulsion between the cation and the nearest carbonyl groups, and the moderate electrostatic repulsion between the coordinating carbonyl groups. A useful strategy to clarify

how selectivity arises is to carry out FEP calculations in which the electrostatic interaction between the carbonyl groups located in different subunits of the channel is artificially turned off (103). The effect of turning off the carbonyl-carbonyl interaction on the calculated free energy is informative because it is intrinsically associated with the local dynamics and fluctuations of the first coordination shell around the cation. For instance, no significant impact on $\Delta\Delta G$ is expected in the case of a locally rigid structure. Conversely, a large change in $\Delta\Delta G$ is indicative of a flexible coordination structure. Remarkably, removing the carbonyl-carbonyl interaction in a fully flexible KcsA channel completely destroys the selectivity of site S_2, which then becomes significantly favorable for Na^+. The relative free energy, originally unfavorable for Na^+ by 5.3 kcal mol^{-1}, becomes favorable by 2.9 kcal mol^{-1}, with a net loss of 8.2 kcal mol^{-1} in selectivity, when the repulsive interactions between the backbone carbonyl is turned off. To further assess the influence of the architectural rigidity of the protein relative to the local carbonyl interactions, additional FEP calculations were performed, keeping all atoms fixed except those forming the selectivity filter (i.e., the backbone atom of residues Thr-74 to Asp-78). Remarkably, despite the frozen protein structure surrounding the selectivity filter, the FEP calculations for site S_2 show that the relative free energy decreases from 6.7 to 0.9 kcal mol^{-1} when the carbonyl repulsion in the selectivity filter is removed. There is a loss of almost 6 kcal mol^{-1} of selectivity for K^+ over Na^+ even if only the backbone of the selectivity filter is allowed to move dynamically and fluctuate. The FEP calculations show that any architectural subangstrom rigidity of the protein conferred by the highly conserved residues surrounding the selectivity filter is not a key factor in making the channel selective for K^+ over Na^+. Further computations with a reduced model system representing the binding site S_2 demonstrate that ion selectivity is a robust feature of such a flexible fluctuating pore lined by carbonyl groups (103).

Control of Selectivity by Dynamical and Electrostatic Properties

Ionic selectivity in K^+ channels is controlled by the intrinsic local physical properties of the ligands coordinating the cation in the binding site (103). Such a perspective bears some similarities to the treatment of ionic selectivity elaborated by Eisenman and colleagues, who identified the strength of the electric field arising from the ligands coordinating the cation in a binding site as a key factor in determining selectivity (40, 41, 120, 128). To illustrate this, a simple toy model with eight carbonyl-like (C=O) dipoles surrounding a central cation fluctuating freely inside a sphere with a radius of 3.5 Å was considered. The results reveal that such a simple system is naturally and optimally selective for K^+, demonstrating that selectivity for K^+ over Na^+ is possible without any architectural rigidity preventing the coordinating ligands from collapsing onto a smaller cation. Selectivity for K^+ or for Na^+ requires different chemical functionalities to favorably coordinate the cation. This conclusion is also consistent with an examination of the

amino acid sequence of ionic channels in various genomes, which suggests that no biological channels selective for Na^+ have evolved by refining the geometry of a KcsA-like pore lined by backbone carbonyl groups (64). One possibility to achieve Na^+ selectivity (although there are certainly others) would be to introduce a salt-bridge formed by the association of two charged residues directly into the pore. Intriguingly, the amino acids identified to be essential for the selectivity of Na^+ channels include the highly conserved DEKA locus from four different protein domains (61, 64).

CATION BINDING SITES

Detailed information about energetically favorable binding sites along the permeation pathway is essential to understand the ion conduction process at the molecular level. Results from both X-ray crystallography (131, 135) and MD free energy simulations (7, 17) show that specific cation binding sites are disposed along the selectivity filter of KcsA (Figure 1). A complete characterization of these binding sites, structural and energetics, is of paramount importance to understand ion permeation.

External S_0 Binding Site

The binding site S_0, located on the extracellular side of the channel, is particularly intriguing. A cation moving from site S_0 to site S_1 is in the process of being progressively dehydrated. For this reason, this site is of great interest (although perhaps more difficult to characterize). The binding site was not detected in the initial structure of KcsA (39) at 3.2 Å resolution, but a spontaneous concerted transition to a configuration with a K^+ occupying S_0 was first observed during all-atom MD trajectory of KcsA in a lipid membrane based on this crystallographic structure (16). The site was not detected in the subsequent higher resolution structures (95, 132) based on the initial construct, but it was observed in the structure at 2.0 Å resolution crystalized with a Fab antibody fragment. This suggests that detection of ion occupancy in site S_0 in KcsA crystals is not simply a matter of resolution. Examination of the lattice packing in those protein crystals suggests a possible explanation: There is a head-to-head interaction between neighboring channels (their extracellular entrance facing one another), and occupancy of S_0 by a K^+ is energetically prohibitive because of ion-ion repulsion (Figure 4, see color insert). The K^+ in site S_0 is closer to the protein by approximately 1.5 Å along the channel axis in the calculations (17) relative to the position determined in the high-resolution X-ray structure (135). In the computations, a K^+ in S_0 is partially hydrated by three to four water molecules and transiently coordinated by the carbonyl oxygens of Tyr-78, whereas the cation appears to be more fully hydrated in the X-ray structure. The significance of these differences is unclear. The computations attempt to simulate a channel in a bilayer membrane solvated by an aqueous solution at room temperature using an approximate potential function (17), whereas the diffraction

data report detailed experimental measurements on the cation occupancy, but for protein crystals at liquid nitrogen temperature and solvated by an aqueous solution including 40% polyethyleneglycol (PEG) for cryo-protection (135). The impact of fast-freezing protein crystals on fine atomic details is difficult to assess (56, 57). There are indications that the packing and configuration of charged side chains in protein crystals can be quite sensitive to temperature (72), and perhaps such a conclusion applies to hydrated ions near channel vestibules as well. Although MD simulations are burdened by several approximations, notably the neglect of induced polarizability near small ions, similar calculations have accurately predicted the position of water molecules in aquaporins (34, 121).

Hydrated Cation in Vestibular Cavity

A solvated K^+ surrounded by exactly eight water molecules is observed at the center of the vestibular cavity in the X-ray structure (135). But other cations (Na^+, Rb^+, Cs^+, and Tl^+) in the cavity do not display a similarly ordered hydration structure (134). These observations are intriguing. However, it is unknown whether the observed average density is representative of the typical hydration of a cation in the channel cavity. The effect of flash-freezing protein crystals on the structure of water is different for wide and narrow solvent-filled regions (125), and this should be carefully assessed in the case of K^+ channel crystals. Furthermore, the pore axis corresponds to an axis of crystallographic symmetry in the structure cocrystalized with Fab antibody fragment (135). As a result, there is a fourfold averaging of the hydration structure around the cation. In MD simulations (performed at room temperature), the hydration shell surrounding the K^+ in the cavity is similar to what it would be in bulk solution (16), with a hydration number fluctuating transiently between six and nine water molecules. The hydration structure seen in MD simulation is in general accord with results from experimental studies based on neutron and X-ray scattering on aqueous ionic solution (42, 67, 100, 104, 105; for a recent review see Reference 99). Therefore, more work is required to understand the hydration structure around a cation located inside the cavity of a K^+ channel.

Multi-Ion Energetics

During the conduction process, ion movements are expected to take place in a highly concerted way, as the K^+ in the pore undergo sudden hopping transitions between various multi-ion configurations. For this reason, it is important to characterize not only the position of the cation binding sites but also the relative stability of the multi-ion configurations and the free energy barriers between them. Using a systematic search procedure, the thermodynamical stability of all the possible ways to distribute any number of K^+ among the four cation binding sites located within the narrow selectivity filter (S_1, S_2, S_3, and S_4) was estimated with FEP simulations (7). Only a small subset of occupancy states were energetically allowed, the [S_1, S_3] and [S_2, S_4] configurations (7), with the two K^+ separated by

one water molecule occupying the selectivity filter. Spontaneous occurrences of such configurations were also observed in several MD simulations of KcsA (16, 54, 118). Diffraction data on KcsA are consistent with these configurations (95), although lattice interactions may have had some impact on the relative stability of the multi-ion configuration (see above). The most compelling experimental evidence for the multi-ion configuration came from diffraction data with a mutant of the KcsA channel (T75C) with altered ion distribution in the selectivity filter (131). Several lines of evidence from the computations indicate that the configurations with three K^+ are [cavity, S_3, S_1] and [S_4, S_2, S_0]. Notably, there appears to be some repulsive interaction opposing the simultaneous occupancy of the cavity and site S_4, or sites S_1 and S_0. For example, absence of a K^+ in the cavity has a strong effect on the relative stability of the [S_1, S_3] and [S_2, S_4] configurations (55). Although consistent with available data, these computational results have yet to be tested directly by experiments. Calculations based on simplified semimicroscopicmodels may help clarify the origin of the factors dominating the energy of multi-ion configurations (48). Detailed kinetic analysis of ion-flux data with different ions and rapid pore blockers may also provide clues about the multi-ion configurations governing the ion conduction process (78, 122). Additional information, possibly from X-ray structures of other K^+ channels (77), might help to better characterize the cation binding sites. However, the delicate balance of attractive and repulsive forces may be slightly different for various K^+ channels.

Selectivity of the Binding Sites

FEP computations indicate that the selectivity of the cation binding sites along the pore is different (7, 17, 103). The most selective appears to be site S_2, located in the center of the pore. Sites S_1 and S_3 display moderate selectivities, whereas S_0 and S_4 are not selective. The results of punchthrough experiments with Na^+ on the intracellular side can be interpretedas evidence of Na^+ blocking the pore by entering the cavity (102), although it is also possible that Na^+ is blocking the pore by occupying site S_4. The vestibular cavity on the intracellular side does not display any selectivity in the computations, but the hydration structure around cations seen in X-ray diffraction depends on the ion type (134, 135). Comparison of MD trajectories with different cations in the KcsA channel suggests that K^+, Rb^+, and Cs^+ behave in a similar way, but that the differenceis more pronounced in the case of Na^+ (38). Diffraction data indicate that Rb^+ and Cs^+ do not easily occupy site S_2 in KcsA (95, 133, 135) (although ion-flux measurements suggest that this might be different in Shaker, see Reference 122). How sensitive these observations are to the low temperature of the crystals is still unknown. In the future, it would be of interest to characterize the relative stability of those cationsin the various binding sites at different temperatures using FEP computations. More accurate quantum mechanical electronic structure computations might help ascertain the validity of the conclusions from MD simulations based on all-atom force fields (12, 53; see 27 for review).

PORE BLOCKERS AND INHIBITORS

Quaternary Ammonium and Other Compounds

An important fraction of the present information about the function of K^+ channels has been deduced from studies with quaternary ammonium (QA) pore blockers, such as tetramethylammonium (TMA), tetraethylammonium (TEA), tetrabutylammonium (TBA), and related alkyl derivatives (8, 9, 10, 44, 129). QAs act by blocking the permeation pathway, occluding the movement of K^+ ions through the pore. Nearly all K^+ channels are blocked by QAs on the intracellular side. In contrast, some K^+ channels are blocked by TEA on the extracellular side, whereas others are not. The affinity of extracellular TEA blockade is enhanced by the presence of aromatic residues located near the extracellular mouth of the pore (60, 74, 90). By virtue of their ability to act as sensors of the pore of K^+ channels, these classical blockers are important tools in electrophysiological studies of biological membranes.

A number of computational studies have investigated the interactions of classical QA blockers with the KcsA channel (31, 53, 84, 86). Computations of the interactions of TEA with the KcsA channel have clarified the origin of the important aromatic residue near the pore extracellular entrance (31, 53, 84). The studies generally indicate that TEA would occupy the S_0 cation binding site observed in the X-ray structure (135) and in PMF computations (17). One consequence is that extracellular binding of TEA may drive the multi-ion system toward a configuration with two K^+ occupying sites S_4 and S_2 and a TEA in site S_0 (with each ion pair separated by a single water molecule). Recently, studies on classical blockers have been extended to examine the interaction of bupivacaine with a model of the Kv1.5 channel in the open state (85).

Toxin Peptide Inhibitors

Toxin inhibitors are small proteins that bind at the pore entryway on the extracellular side between the four subunits, thus blocking the channel. Their high specificity makes them powerful tools for characterizing K^+ channels structurally. Scorpion toxins have been used to identify the pore region of K^+ channels (88, 89), elucidate the topology of the extracellular face of the channel (50, 62, 109), assign the functional sidedness of the proton activation of KcsA (59), and aid in the design of a promising strategy to target lymphocytes (110). The general architecture of the extracellular face of the Shaker K^+ channel deduced from the results of thermodynamic mutant cycles with agitoxin (109) was strikingly consistent with the X-ray structure of the KcsA channel (87). But there is yet no high-resolution structure of a toxin in complex with a K^+ channel.

A computational approach was developed to determine and refine models of the structure of agitoxin in complex with the Shaker K^+ channel on the basis of mutant cycle data (43); the change in binding free energies upon site-directed mutations was calculated using PB computations and compared with experimental data to

rank and assess the validity of the large number of models generated. The interaction of kappa-conotoxin-PVIIA with the Shaker K^+ channel pore was simulated by MD (96). BD has been a popular approach to simulate the association and interactions of toxins with the extracellular vestibule of K^+ channel. This method has been applied to toxin Lq2 (33) and maurotoxin (45). The interaction of agitoxin, charybdotoxin, and iberiotoxin with various K^+ channels was investigated byusing atomic models and energy minimization, and the factors responsible for the selectivity between different voltage-gated and Maxi-K channels were explored (46). The interaction between ScyTx and the small conductance calcium-activated K^+ channel has been investigated by using docking and a combination of MD and PB computations (127).

GATING

Intracellular Gating

Characterizing the molecular determinants of gating is a challenge, and despite the remarkable progress, numerous fundamental questions remain unresolved. Results from the bacterial channels provide some important clues. The full-length KcsA channel is mostly closed at neutral pH, but it can be stabilized in the open state at low intracellular pH (59); the X-ray structures (39, 135) (with their C-terminals truncated) correspond to the closed nonconducting state (107, 113). A similar closed form is revealed by the X-ray structure of a bacterial inward-rectifier K^+ channel, the KirBac (77). Data from ESR with site-specific spin-labels suggest that channel gating involves the movements of the inner helices, which presumably lead to the opening of the pore on the intracellular side (107). MD trajectories, biased to enforce an opening of the intracellular gate, revealed the propensity of the innerhelices to bend near a highly conserved glycine residue (14, 20). A similar helix bending is observed in the X-ray structure of the calcium-activated MthK channel (68), which was crystallized in its open state at high Ca^{2+} concentrations. Whether such helical distortion is a completely general mechanism among K^+ channels is an open question (35, 71, 124).

Gating by the Selectivity Filter?

Some indications of the selectivity filter's ability to distort areprovided by a crystallographic X-ray structure of the KcsA K^+ channel determined with 2 mM KCl and 148 mM NaCl (133, 135). In this so-called low K^+ structure, the orientation of the carbonyl group of Val-76 is significantly tilted relative to the structure determined at high K^+ concentrations. This result highlights the flexibility of the selectivity filter, showing that its exact conformation depends on the nature of its interactions with bound cations. In addition, spontaneous reorientation transitions of the Val76-Gly77 peptide linkage have been observed in several independent MD studies of KcsA based on different force fields and simulation methodologies

(16, 38, 123), as well as in simulations of Kir6.2 (25) and KirBac (36). This strongly suggests that the important backbone flexibility of the selectivity filter conferred by the glycine residues and the existence of conformational states of broken symmetry may be a genuine property of the selectivity filter of K^+ channels. The distorted conformation observed in MD and X-ray studies is not, however, identical. In the low K^+ X-ray structure, the Val-76 amide plane of the four subunits is tilted simultaneously by approximately $45°$ in a fourfold symmetric manner, and the selectivity filter remains in the vicinity of the structure determined with 150 mM KCl. In the simulations, the fourfold symmetry of the selectivity filter is lost. The relation of such distorted conformation with the ability of the selectivity filter to adopt long-lived nonconducting blocked states, such as those observed in single-channel recordings, is intriguing and requires further investigation.

CONCLUSION

The remarkable progress in understanding ion permeation through K^+ channels in the past few years enables us to formulate new questions to continue to refine our view of these systems. Many of the basic features of ion conduction and selectivity of K^+ channels seem to be solidly established. Nonetheless, despite the detailed information provided by experiments (95, 131, 134, 135), several questions about the relative stability of the multi-ion configurations and the free energy barrier between them remain unresolved. Of particular interest is a quantitative characterization of the repulsive interaction between ions in the vestibular cavity and those in the selectivity filter. Similarly, a number of fundamental questions concerning the relative selectivity of the various binding sites and the vestibular cavity need to be addressed. A useful strategy is to attack the problem from a broad perspective, for example, by comparing the results of MD simulations for different biological channels built on the basis of sequence homology with the known X-ray structures (25, 36, 116). Continued efforts at combining and contrasting the results from atomic models with the information obtained from a wide range of structural, biophysical, and functional measurements will help develop an increasingly detailed perspective of ion permeation in K^+ channels.

The *Annual Review of Biophysics and Biomolecular Structure* is online at
http://biophys.annualreviews.org

LITERATURE CITED

1. Alcayaga C, Cecchi X, Alvarez O, Latorre R. 1989. Streaming potential measurements in Ca^{2+}-activated K^+ channels from skeletal and smooth muscle. Coupling of ion and water fluxes. *Biophys. J.* 55:367–71

2. Allen M, Tildesley D. 1989. *Computer Simulation of Liquids*. Oxford, UK: Oxford Sci./Clarendon

3. Allen TW, Andersen OS, Roux B. 2004. On the importance of atomic fluctuations, protein flexibility and solvent

in ion permeation. *J. Gen. Physiol.* In press

4. Allen TW, Bliznyuk A, Rendell A, Kuyucak S, Chung SH. 2000. The potassium channel: structure, selectivity and diffusion. *J. Chem. Phys.* 112:8191–204

5. Allen TW, Chung SH. 2001. Brownian dynamics of an open-state KcsA potassium channel. *Biophys. Biochim. Acta* 1515:83–91

6. Allen TW, Kuyucak S, Chung SH. 1999. Molecular dynamics study of the KcsA potassium channel. *Biophys. J.* 77:2502–16

7. Åqvist J, Luzhkov VB. 2000. Ion permeation mechanism of the potassium channel. *Nature* 404:881–84

8. Armstrong CM. 1969. Inactivation of the potassium conductance and related phenomena caused by quaternary ammonium ion injection in squid axons. *J. Gen. Physiol.* 54:553–75

9. Armstrong CM. 1968. Induced inactivation of the potassium permeability of squid axon membranes. *Nature* 219:1262–63

10. Armstrong CM. 1971. Interaction of tetraethylammonium ion derivatives with the potassium channels of giant axons. *J. Gen. Physiol.* 58:413–37

11. Armstrong CM. 2003. Voltage-gated K channels. *Science STKE* 188:re10

12. Ban F, Kusalik P, Weaver DF. 2004. Density functional theory investigations on the chemical basis of the selectivity filter in the K^+ channel protein. *J. Am. Chem. Soc.* 126:4711–16

13. Becker OM, MacKerell AD, Roux B, Watanabe M. 2001. *Computational Biochemistry and Biophysics*. New York: Marcel Dekker

14. Beckstein O, Biggin PC, Bond P, Bright JN, Domene C, et al. 2003. Ion channel gating: insights via molecular simulations. *FEBS Lett.* 555:85–90

15. Berg JM, Tymoczko JL, Stryer L. 2002. *Biochemistry*. New York: Freeman. 5th ed.

16. Bernèche S, Roux B. 2000. Molecular dynamics of the KcsA K(+) channel in a bilayer membrane. *Biophys. J.* 78:2900–17

17. Bernèche S, Roux B. 2001. Energetics of ion conduction through the K^+ channel. *Nature* 414:73–77

18. Bernèche S, Roux B. 2003. A microscopic view of ion conduction through the KcsA K^+ channel. *Proc. Natl. Acad. Sci. USA* 100:8644–48

19. Bezanilla F, Armstrong CM. 1972. Negative conductance caused by entry of sodium and cesium ions into the potassium channels of squid axons. *J. Gen. Physiol.* 60:588–608

20. Biggin PC, Sansom MS. 2002. Open-state models of a potassium channel. *Biophys. J.* 83:1867–76

21. Biggin PC, Smith GR, Shrivastava I, Choe S, Sansom MS. 2001. Potassium and sodium ions in a potassium channel studied by molecular dynamics simulations. *Biochim. Biophys. Acta* 1510:1–9

22. Burykin A, Kato M, Warshel A. 2003. Exploring the origin of the ion selectivity of the KcsA potassium channel. *Protein Struct. Funct. Gen.* 52:412–26

23. Burykin A, Schutz C, Villa J, Warshel A. 2002. Simulations of ion current in realistic models of ion channels: the KcsA potassium channel. *Protein Struct. Funct. Gen.* 47:265–80

24. Capener CE, Kim HJ, Arinaminpathy Y, Sansom MS. 2002. Ion channels: structural bioinformatics and modelling. *Hum. Mol. Genet.* 11:2425–33

25. Capener CE, Proks P, Ashcroft FM, Sansom MS. 2003. Filter flexibility in a mammalian K channel: models and simulations of Kir6.2 mutants. *Biophys. J.* 84:2345–56

26. Capener CE, Shrivastava IH, Ranatunga KM, Forrest LR, Smith GR, Sansom MS. 2000. Homology modeling and molecular dynamics simulation studies of an inward rectifier potassium channel. *Biophys. J.* 78:2929–42

27. Carloni P, Rothlisberger U, Parrinello M. 2002. The role and perspective of ab initio molecular dynamics in the study of biological systems. *Acc. Chem. Res.* 35:455–64

28. Chung S, Allen T, Kuyucak S. 2002. Modeling diverse range of potassium channels with Brownian dynamics. *Biophys. J.* 83:263–77

29. Compoint M, Carloni P, Ramseyer C, Girardet C. 2004. Molecular dynamics study of the KcsA channel at 2.0-A resolution: stability and concerted motions within the pore. *Biochim. Biophys. Acta* 1661:26–39

30. Cortes D, Cuello L, Perozo E. 2001. Molecular architecture of full-length KcsA: role of cytoplasmic domains in ion permeation and activation gating. *J. Gen. Physiol.* 117:165–80

31. Crouzy S, Bernèche S, Roux B. 2001. Extracellular blockade of K^+ channels by TEA: results from molecular dynamics simulations of the KcsA channel. *J. Gen. Physiol.* 118:207–17

32. Cuello LG, Cortes DM, Perozo E. 2004. KvAP voltage-dependent K^+ channel in a lipid bilayer. *Science* 306:491–95

33. Cui M, Shen J, Briggs JM, Luo X, Tan X, et al. 2001. Brownian dynamics simulations of interaction between scorpion toxin Lq2 and potassium ion channel. *Biophys. J.* 80:1659–69

34. deGroot BL, Grubmuller H. 2001. Water permeation across biological membranes: mechanism and dynamics of aquaporin-1 and GlpF. *Science* 294:2353–57

35. del Camino D, Holmgren M, Liu Y, Yellen G. 2000. Blocker protection in the pore of a voltage-gated K^+ channel and its structural implications. *Nature* 403:321–35

36. Domene C, Grottesi A, Sansom MS. 2004. Filter flexibility and distortion in a bacterial inward rectifier K^+ channel: simulation studies of KirBac1.1. *Biophys. J.* 87:256–67

37. Domene C, Haider S, Sansom MS. 2003. Ion channel structures: a review of recent progress. *Curr. Opin. Drug Discov. Dev.* 6:611–19

38. Domene C, Sansom MS. 2003. Potassium channel, ions, and water: simulation studies based on the high resolution X-ray structure of KcsA. *Biophys. J.* 85:2787–800

39. Doyle D, Morais Cabral J, Pfuetzner RA, Kuo A, Gulbis JM, et al. 1998. The structure of the potassium channel: molecular basis of K^+ conduction and selectivity. *Science* 280:69–77

40. Eisenman G. 1962. Cation selective electrodes and their mode of operation. *Biophys. J.* 2(Suppl. 2):259–323

41. Eisenman G, Horn R. 1983. Ionic selectivity revisited: the role of kinetic and equilibrium processes in ion permeation through channels. *J. Membr. Biol.* 76:197–225

42. Enderby JE. 1983. Neutron scattering from ionic solutions. *Annu. Rev. Phys. Chem.* 34:155–85

43. Eriksson MA, Roux B. 2002. Modeling the structure of agitoxin in complex with the Shaker K^+ channel: a computational approach based on experimental distance restraints extracted from thermodynamic mutant cycles. *Biophys. J.* 83:2595–609

44. French RJ, Shoukimas JJ. 1981. Blockage of squid axon potassium conductance by internal tetra-N-alkylammonium ions of various sizes. *Biophys. J.* 34:271–91

45. Fu W, Cui M, Briggs JM, Huang X, Xiong B, et al. 2002. Brownian dynamics simulations of the recognition of the scorpion toxin maurotoxin with the voltage-gated potassium ion channels. *Biophys. J.* 83:2370–85

46. Gao YD, Garcia ML. 2003. Interaction of agitoxin2, charybdotoxin, and iberiotoxin with potassium channels: selectivity between voltage-gated and Maxi-K channels. *Proteins* 52:146–54

47. Garman E. 1999. Cool data: quantity AND quality. *Acta Crystallogr. D* 55:1641–53

48. Garofoli S, Jordan PC. 2003. Modeling permeation energetics in the KcsA potassium channel. *Biophys. J.* 84:2814–30

49. Giorgetti A, Carloni P. 2003. Molecular modeling of ion channels: structural predictions. *Curr. Opin. Chem. Biol.* 7:150–56

50. Goldstein SA, Pheasant DJ, Miller C. 1994. The charybdotoxin receptor of a Shaker K$^+$ channel: peptide and channel residues mediating molecular recognition. *Neuron* 12:1377–88

51. Gross A, Columbus L, Hideg K, Altenbach C, Hubbell WL. 1999. Structure of the KcsA potassium channel from Streptomyces lividans: a site-directed spin labeling study of the second transmembrane segment. *Biochemistry* 38:10324–35

52. Gross A, Hubbell WL. 2002. Identification of protein side chains near the membrane-aqueous interface: a site-directed spin labeling study of KcsA. *Biochemistry* 41:1123–28

53. Guidoni L, Carloni P. 2002. Potassium permeation through the KcsA channel: a density functional study. *Biochim. Biophys. Acta* 1563:1–6

54. Guidoni L, Torre V, Carloni P. 1999. Potassium and sodium binding to the outer mouth of the K$^+$ channel. *Biochemistry* 38:8599–604

55. Guidoni L, Torre V, Carloni P. 2000. Water and potassium dynamics inside the KcsA K(+) channel. *FEBS Lett.* 477:37–42

56. Halle B. 2002. Flexibility and packing in proteins. *Proc. Natl. Acad. Sci. USA* 99:1274–79

57. Halle B. 2004. Biomolecular cryocrystallography: structural changes during flashcooling. *Proc. Natl. Acad. Sci. USA* 101:4793–98

58. Heginbotham L, Abramson T, MacKinnon R. 1992. A functional connection between the pores of distantly related ion channels as revealed by mutant K$^+$ channels. *Science* 258:1152

59. Heginbotham L, LeMasurier M, Kolmakova-Partensky L, Miller C. 1999. Single Streptomyces lividans K(+) channels: functional asymmetries and sidedness of proton activation. *J. Gen. Physiol.* 114:551–60

60. Heginbotham L, MacKinnon R. 1992. The aromatic binding site for tetraethylammonium ion on potassium channels. *Neuron* 8:483–91

61. Heinemann SH, Terlau H, Stuhmer W, Imoto K, Numa S. 1992. Calcium channel characteristics conferred on the sodium channel by single mutations. *Nature* 356:441–43

62. Hidalgo P, MacKinnon R. 1995. Revealing the architecture of a K$^+$ channel pore through mutant cycles with a peptide inhibitor. *Science* 268:307–10

63. Hille B. 1973. Potassium channels in myelinated nerve: selective = permeability to small cations. *J. Gen. Physiol.* 61:669–86

64. Hille B. 2001. *Ionic Channels of Excitable Membranes*. Sunderland, MA: Sinauer. 3rd ed.

65. Hille B, Armstrong CM, MacKinnon R. 1999. Ion channels: from idea to reality. *Nat. Med.* 5:1105–19

66. Hodgkin AL, Keynes RD. 1955. The potassium permeability of a giant nerve fibre. *J. Physiol.* 128:61–88

67. Howell I, Neilson GW, Chieux P. 1991. Neutron-diffraction studies of ions in aqueous-solution. *J. Mol. Struct.* 250:281–89

68. Jiang YX, Lee A, Chen JY, Cadene M, Chait BT, MacKinnon R. 2002. Crystal structure and mechanism of a calciumgated potassium channel. *Nature* 417:515–22

69. Jiang YX, Lee A, Chen JY, Cadene M, Chait BT, MacKinnon R. 2002. The open pore conformation of potassium channels. *Nature* 417:523–26

70. Jiang YX, Lee A, Chen JY, Ruta V, Cadene M, et al. 2003. X-ray structure of a voltage-dependent K$^+$ channel. *Nature* 423:33–41

71. Johnson JP Jr, Zagotta WN. 2001. Rotational movement during cyclic nucleotide-gated channel opening. *Nature* 412: 917–21

72. Juers DH, Matthews BW. 2001. Reversible lattice repacking illustrates the temperature dependence of macromolecular interactions. *J. Mol. Biol.* 311:851–62

73. Karplus M, Petsko GA. 1990. Molecular dynamics simulations in biology. *Nature* 347:631–39

74. Kavanaugh MP, Hurst RS, Yakel J, Varnum MD, Adelman JP, North RA. 1992. Multiple subunits of a voltage-dependent potassium channel contribute to the binding site for tetraethylammonium. *Neuron* 8:493–97

75. Kelly BL, Gross A. 2003. Potassium channel gating observed with site-directed mass tagging. *Nat. Struct. Biol.* 10:280–84

76. Khodakhah K, Melishchuk A, Armstrong CM. 1997. Killing K channels with TEA+. *Proc. Natl. Acad. Sci. USA* 94: 13335–38

77. Kuo A, Gulbis JM, Antcliff JF, Rahman T, Lowe ED, et al. 2003. Crystal structure of the potassium channel KirBac1.1 in the closed state. *Science* 300:1922–26

78. Kutluay E, Roux B, Heginbotham L. 2004. Intracellular blockade of KcsA by TEA. *Biophys. J.* In press

79. LeMasurier M, Heginbotham L, Miller C. 2001. KcsA: It's a potassium channel. *J. Gen. Physiol.* 118:303–14

80. Liu Y, Sompornpisut P, Perozo E. 2001. Structure of the KcsA channel intracellular gate in the open state. *Nat. Struct. Biol.* 8:883–87

81. Loboda A, Melishchuk A, Armstrong CM. 2001. Dilated and defunct K channels in the absence of K+. *Biophys. J.* 80:2704–14

82. Luzhkov VB, Åqvist J. 2000. A computational study of ion binding and protonation states in the KcsA potassium channel. *Biochim. Biophys. Acta* 1481:360–70

83. Luzhkov VB, Åqvist J. 2001. K(+)/Na(+) selectivity of the KcsA potassium channel from microscopic free energy perturbation calculations. *Biochim. Biophys. Acta* 1548:194–202

84. Luzhkov VB, Åqvist J. 2001. Mechanisms of tetraethylammonium ion block in the KcsA potassium channel. *FEBS Lett.* 495:191–96

85. Luzhkov VB, Nilsson J, Arhem P, Åqvist J. 2003. Computational modelling of the open-state Kv 1.5 ion channel block by bupivacaine. *Biochim. Biophys. Acta* 1652:35–51

86. Luzhkov VB, Osterberg F, Åqvist J. 2003. Structure-activity relationship for extracellular block of K+ channels by tetraalkylammonium ions. *FEBS Lett.* 554:159–64

87. MacKinnon R, Cohen S, Kuo A, Lee A, Chait B. 1998. Structural conservation in prokaryotic and eukaryotic potassium channels. *Science* 280:106–9

88. MacKinnon R, Heginbotham L, Abramson T. 1990. Mapping the receptor site for charybdotoxin, a pore-blocking potassium channel inhibitor. *Neuron* 5:767–71

89. MacKinnon R, Miller C. 1989. Mutant potassium channels with altered binding of charybdotoxin, a pore-blocking peptide inhibitor. *Science* 245:1382–85

90. MacKinnon R, Yellen G. 1990. Mutations affecting TEA blockade and ion permeation in voltage-activated K+ channels. *Science* 250:276–79

91. Mashl RJ, Tang Y, Schnitzer J, Jakobsson E. 2001. Hierarchical approach to predicting permeation in ion channels. *Biophys. J.* 81:2473–83

92. Melishchuk A, Loboda A, Armstrong CM. 1998. Loss of shaker K channel conductance in 0 K+ solutions: role of the voltage sensor. *Biophys. J.* 75:1828–35

93. Miller C. 2001. See potassium run. *Nature* 414:23–24

94. Miloshevsky GV, Jordan PC. 2004. Permeation in ion channels: the interplay

of structure and theory. *Trends Neurosci.* 27:308–14

95. Morais-Cabral J, Zhou Y, MacKinnon R. 2001. Energetic optimization of ion conduction rate by the K^+ selectivity filter. *Nature* 414:37–42

96. Moran O. 2001. Molecular simulation of the interaction of kappa-conotoxin-PVIIA with the Shaker potassium channel pore. *Eur. Biophys. J.* 30:528–36

97. Mullins LJ. 1959. An analysis of conductance changes in squid axon. *J. Gen. Physiol.* 42:1013–35

98. Mullins LJ. 1960. An analysis of pore size in excitable membranes. *J. Gen. Physiol.* 43:105–17

99. Neilson GW, Mason PE, Ramos R, Sullivan D. 2001. Neutron and X-ray scattering studies of hydration in aqueous solution. *Philos. Trans. R. Soc. London Ser. A* 359:1595–91

100. Neilson GW, Skipper NT. 1985. K^+ coordination in aqueous-solution. *Chem. Phys. Lett.* 114:35–38

101. Neyton J, Miller C. 1988. Discrete Ba^{2+} block as a probe of ion occupancy and pore structure in the high-conductance Ca^{2+}-activated K^+ channel. *J. Gen. Physiol.* 92:569–86

102. Nimigean CM, Miller C. 2002. Na(+) block and permeation in a K(+) channel of known structure. *J. Gen. Physiol.* 120:323–35

103. Noskov S, Berneche S, Roux B. 2004. Control of ion selectivity by electrostatic and dynamic properties of carbonyl ligands. *Nature* 431:830–34

104. Ohtaki H, Fukushima N. 1992. A structural study of saturated aqueous-solutions of some alkali-halides by X-ray-diffraction. *J. Solut. Chem.* 21:23–38

105. Ohtaki H, Radnai T. 1993. Structure and dynamics of hydrated ions. *Chem. Rev.* 93:1157–204

106. Pauling L. 1960. *Nature of the Chemical Bond and Structure of Molecules and Crystals.* Ithaca, NY: Cornell Univ. Press. 3rd ed.

107. Perozo E, Cortes D, Cuello L. 1999. Structural rearrangements underlying K^+-channel activation gating. *Science* 285:73–78

108. Ranatunga KM, Shrivastava IH, Smith GR, Sansom MS. 2001. Side-chain ionization states in a potassium channel. *Biophys. J.* 80:1210–19

109. Ranganathan R, Lewis JH, MacKinnon R. 1996. Spatial localization of the K^+ channel selectivity filter by mutant cycle-based structure analysis. *Neuron* 16:131–39

110. Rauer H, Lanigan MD, Pennington MW, Aiyar J, Ghanshani S, et al. 2000. Structure-guided transformation of charybdotoxin yields an analog that selectively targets Ca(2+)-activated over voltage-gated K(+) channels. *J. Biol. Chem.* 275:1201–8

111. Roux B. 2002. Theoretical and computational models of ion channels. *Curr. Opin. Struct. Biol.* 12:182–89

112. Roux B, Allen TW, Bernèche S, Im W. 2004. Theoretical and computational models of biological ion channels. *Q. Rev. Biophys.* 37:15–103

113. Roux B, Bernèche S, Im W. 2000. Ion channels, permeation and electrostatics: insight into the function of KcsA. *Biochemistry* 39:13295–306

114. Roux B, MacKinnon R. 1999. The cavity and pore helices in the KcsA K^+ channel: electrostatic stabilization of monovalent cations. *Science* 285:100–2

115. Roux B, Schulten K. 2004. Computational studies of membrane channels. *Structure* 12:1343–51

116. Sansom MS, Shrivastava IH, Bright JN, Tate J, Capener CE, Biggin PC. 2002. Potassium channels: structures, models, simulations. *Biochim. Biophys. Acta* 1565:294–307

117. Shealy RT, Murphy AD, Ramarathnam R, Jakobsson E, Subramaniam S. 2003. Sequence-function analysis of the K^+-selective family of ion channels using a comprehensive alignment and the KcsA

channel structure. *Biophys. J*. 84:2929–42

118. Shrivastava IH, Sansom MS. 2000. Simulations of ion permeation through a potassium channel: molecular dynamics of KcsA in a phospholipid bilayer. *Biophys. J.* 78:557–70

119. Shrivastava IH, Tieleman DP, Biggin PC, Sansom MS. 2002. K(+) versus Na(+) ions in a K channel selectivity filter: a simulation study. *Biophys. J.* 83:633–45

120. Szabo G, Eisenman G, Laprade R, Ciani SM, Krasne S. 1973. Experimentally observed effects of carriers on the electrical properties of bilayer membranes–equilibrium domain. With a contribution on the molecular basis of ion selectivity. *Membranes* 2:179–328

121. Tajkhorshid E, Nollert P, Jensen MA, Miercke LJ, O'Connell J, et al. 2002. Control of the selectivity of the aquaporin water channel family by global orientational tuning. *Science* 296:525–30

122. Thompson J, Begenisich T. 2003. External TEA block of Shaker K$^+$ channels is coupled to the movement of K$^+$ ions within the selectivity filter. *J. Gen. Physiol.* 122:239–46

123. Tieleman DP, Biggin PC, Smith GR, Sansom MS. 2001. Simulation approaches to ion channel structure-function relationships. *Q. Rev. Biophys*. 34:473–561

124. Webster SM, del Camino D, Dekker JP, Yellen G. 2004. Intracellular gate opening in Shaker K$^+$ channels defined by high-affinity metal bridges. *Nature* 428:864–68

125. Weik M, Kryger G, Schreurs AM, Bouma B, Silman I, et al. 2001. Solvent behaviour in flash-cooled protein crystals at cryogenic temperatures. *Acta Crystallogr. D* 57:566–73

126. Willis B, Pryor A. 1975. *Thermal Vibrations in Crystallography*. Cambridge, UK: Cambridge Univ. Press

127. Wu Y, Cao Z, Yi H, Jiang D, Mao X, et al. 2004. Simulation of the interaction between ScyTx and small conductance calcium-activated potassium channel by docking and MM-PBSA. *Biophys. J.* 87:105–12

128. Yamashita M, Wesson L, Eisenman G, Eisenberg D. 1990. Where metal ions bind in proteins. *Proc. Natl. Acad. Sci. USA* 87:5648–52

129. Yellen G. 1998. The moving parts of voltage-gated ion channels. *Q. Rev. Biophys.* 31:239–95

130. Yellen G. 2002. The voltage-gated potassium channels and their relatives. *Nature* 419:35–42

131. Zhou M, MacKinnon R. 2004. A mutant KcsA K(+) channel with altered conduction properties and selectivity filter ion distribution. *J. Mol. Biol*. 338:839–46

132. Zhou M, Morais-Cabral JH, Mann S, MacKinnon R. 2001. Potassium channel receptor site for the inactivation gate and quaternary amine inhibitors. *Nature* 411:657–61

133. Zhou Y, MacKinnon R. 2003. The occupancy of ions in the K$^+$ selectivity filter: charge balance and coupling of ion binding to a protein conformational change underlie high conduction rates. *J. Mol. Biol*. 333:965–75

134. Zhou Y, MacKinnon R. 2004. Ion binding affinity in the cavity of the KcsA potassium channel. *Biochemistry* 43:4978–82

135. Zhou Y, Morais-Cabral JH, Kaufman A, MacKinnon R. 2001. Chemistry of ion coordination and hydration revealed by a K$^+$ channel-Fab complex at 2.0 Å resolution. *Nature* 414:43–48
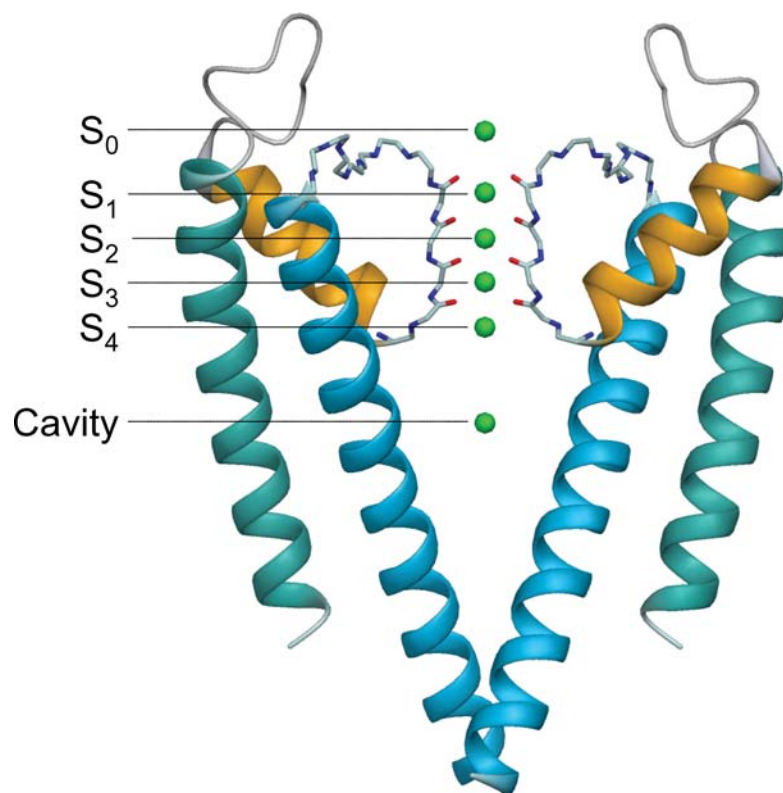
Figure 1   Structure of the KcsA K⁺ channel determined by X-ray crystallography (39). The channel is made of four identical subunits disposed symmetrically around a common axis corresponding to the pore (for the sake of clarity only two of the four monomers are shown). Cation binding sites from both X-ray crystallography (131, 135) and MD free energy simulations (7, 17) are indicated by green spheres.
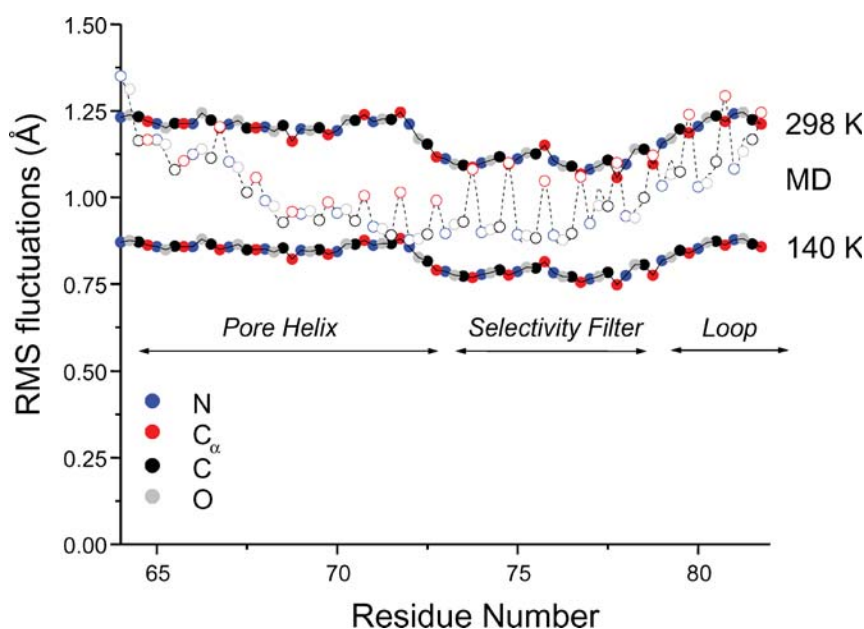
Figure 2   The RMS atomic fluctuations (defined as $\langle<\Delta R^2\rangle^{1/2}$) extracted from the isotropic Debye-Waller crystallographic thermal B-factors of the KcsA channel structure solved at 2.0 Å resolution in complex with a Fab antibody fragment (135) are compared with the results from MD simulations (103). The B-factors of the backbone atoms of the selectivity filter KcsA are in the range of 15 to 20 Å^2. In principle, the B-factors are directly related to the RMS atomic fluctuations with $B = (8\pi^2/3)\langle\Delta R^2\rangle$ (56, 126). However, interpretation of the B-factors requires some care (57) because the crystals were fast-frozen in liquid nitrogen 1 and the diffraction data were obtained under a flow of liquid nitrogen vapor according to a standard protocol (temperature approximately 120 to 140 K). A lower bound to the RMS fluctuations is obtained directly from the experimental B-factors on the basis of the assumption that all thermal motions were quenched infinitely rapidly upon fast-freezing in liquid nitrogen. This lower bound yields RMS atomic fluctuations in the range of 0.8 to 0.9 Å (data identified as 140 K in the figure). However, fast-freezing is not instantaneous on molecular timescales (47, 57). The RMS fluctuations at room temperature (298 K) can be estimated on the basis of the assumption that the small subangstrom librations of the backbone occurring on the picosecond timescale have sufficient time to anneal to the lower temperature upon freezing (140 K). Because the thermal quadratic fluctuations are linearly proportional to the effective temperature in the harmonic approximation, the RMS fluctuations at 298 K can be estimated by scaling the RMS fluctuations at 140 K by $\sqrt{298/140}$. This yields RMS atomic fluctuations in the range of 1.1 to 1.2 Å (data identified as 298 K in the figure). The results from MD trajectory (103), shown as open symbols in the figure, fall between the lower and upper estimates from the crystallographic B-factors.
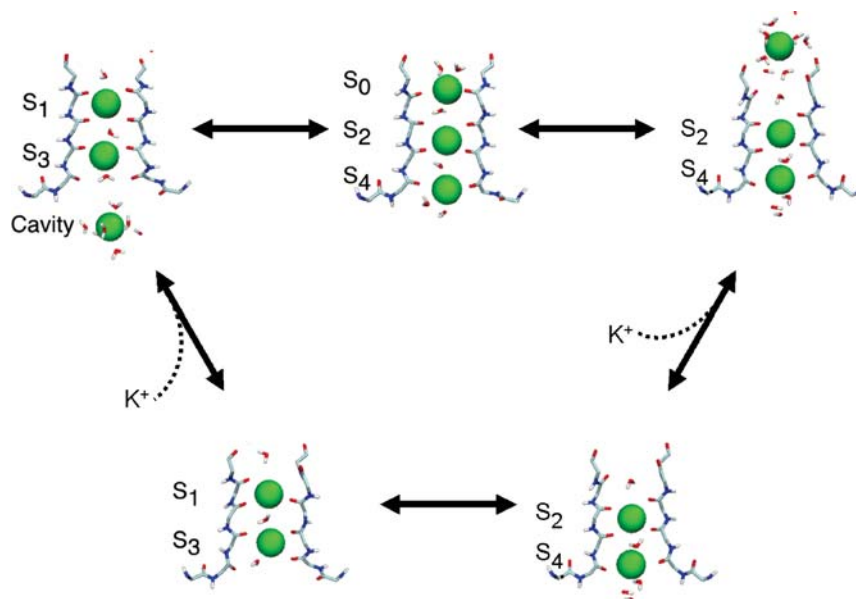
Figure 3 Schematic illustration of the single-file transport mechanism through the selectivity filter of KcsA (17, 18). Ion conduction through KcsA (in the outward direction) is initiated when a K^+ hops in site S_4 from the intracellular vestibular cavity, inducing a concerted transition, to the intermediate state $[S_4, S_2, S_0]$, which is then followed by the rapid dissociation and departure of the outermost K^+ on the extracellular side.
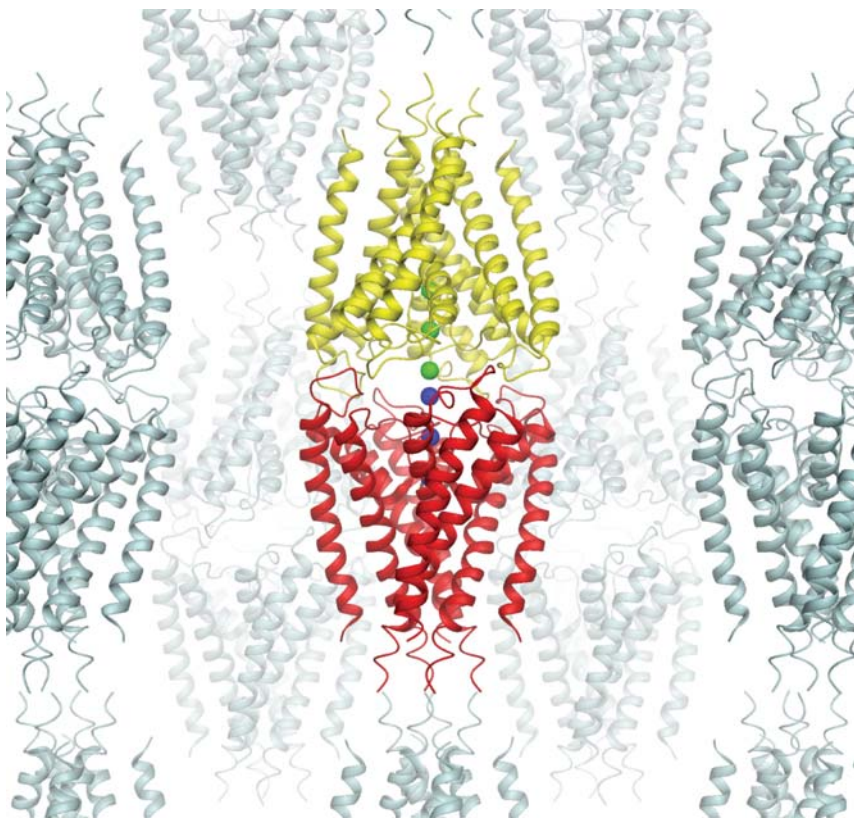
Figure 4 Lattice packing in KcsA crystals from Doyle et al. (39). Ions occupying sites S_4, S_2, and S_0 are represented. The channel in the asymmetric unit is red and its K^+ is blue. The nearest crystallographic neighbor is yellow and its K^+ is green.